



Semnan University



Wall Thermal Inertia Effects of Pulsatile Flow in a Ribbed Tube: A Numerical Approach

Amin Kardgar^{*a}, Davood Domiri Ganji^b

^aDepartment of Mechanical Engineering, University of Mazandaran, Babolsar, Iran.

^bDepartment of Mechanical Engineering, Babol University of Technology, Babol, Iran.

PAPER INFO

Paper history:

Received: 2020-02-24

Revised: 2020-07-01

Accepted: 2020-10-16

Keywords:

Pulsatile flow;
Conjugate heat transfer;
Womersley number;
Wall thickness;
ribbed tube.

ABSTRACT

In the present paper, the heat transfer of pulsatile flow in ribbed tube was investigated numerically by considering the effect of thermal inertia of solid wall thickness. To this purpose, the CVFV technique with collocated grids arrangement was adopted to discretize momentum and energy equations. In order to avoid checker-board of pressure field in numerical simulation, Chow and Rhie interpolation scheme was employed. The well-established SIMPLE (Semi-Implicit Method for Pressure Linked Equations) method was utilized to handle velocity and pressure coupling in the momentum equation. Stone's Strongly Implicit Procedure (SIP) was used to solve the set of individual linear algebraic equations. Womersley number, Reynolds number, velocity amplitude, and wall thickness ratio are four essential parameters that influence heat transfer and Nusselt number in pulsatile flow in a ribbed tube. It was deduced by varying Womersley number Nu does not change. Nu enhances almost 19% by augmentation of wall thickness ratio from 0.125 to 1. It was shown by increasing velocity amplitude from 0.1 to 0.8; Nu reduces almost 4.7%.

DOI: 10.22075/jhmtr.2020.19899.1279

© 2020 Published by Semnan University Press. All rights reserved.

1. Introduction

Pulsating flow heat transfer can occur in natural phenomena like blood flow in veins [1] and in many industrial application like pulse tube and GM cryocooler, Stirling engine, pulse jets, reciprocating engine, and pulse combustors [2][3]. The flow and heat transfer characteristics in pulsating depend on parameters like frequency, Reynolds number, Prandtl number, oscillating amplitude. Extensive investigations have been carried out to study these parameters' effect in hydrodynamics and thermal behavior of such flow by many researchers.

Yuan et al. investigated the effects of wall thickness on heat transfer of pulsatile laminar flow with the boundary condition of constant heat flux within the tube and channel wall. They concluded the pulsatile laminar flow could decrease the average Nusselt number and the effects are significant with high oscillation amplitude, small frequency, low Prandtl number, and large wall thickness heat capacity [4]. Khosravi et al. conducted an experimental study on pressure loss and heat transfer on

pulsatile flow in the heat exchanger with helical geometry. Their results indicated that enhancement in pressure loss compared to steady one is almost 3–7% in pulsatile flow, while Nu number increased up to 39%. Their findings also revealed that Nu number increases sharply at small Reynolds numbers [5]. Li et al. investigated the mechanism of heat transfer of periodic pulsating slot-jet impingement with different waveforms. Their results revealed that T-wave is more contributing to heat transfer enhancement. Their comprehensive results showed that T-wave at large Re with medium frequency could attain a high-efficient heat transfer increase [6].

Many researchers conducted experimental studies actively on pulsating flow. The experimental mensuration was appraised for low pulsating amplitudes in a fully developed region. Heat transfer and the variation of Nu number in pulsatile flow also was investigated experimentally, and the reported results were confusable: Martinelli et al. claimed that the frequency of oscillation did not influence the heat transfer [7]. Genin et al. and

*Corresponding Author: Amin Kardgar, Department of Mechanical Engineering, University of Mazandaran, Babolsar, Iran.
Email: a.kardgar@umz.ac.ir

Barker et al. set up an experimental apparatus to measure heat flux and velocity. They demonstrated that no enhancement was found in heat transfer coefficient in pulsating flow [8]. Park and et al. conducted a numerical simulation and found a slight reduction in heat transfer coefficient in their results [9]. Karamercan investigated oscillation effect on double pipe heat exchanger and concluded that heat transfer and Nu number augmented when only the frequency of pulsation of the flow was greater than a specific value [10].

Several numbers of investigations were also carried out by considering heat conduction in the wall in pulsatile flow. Kardgar and Jafarian studied the effect of heat conduction in axial direction of the solid wall on conjugate heat transfer for oscillating flow at the tube section of Pulse Tube Refrigerator (PTRs) via a numerical method. They claimed that the averaged convection heat transfer coefficient enhances from 5.97 to 28.45 by rising Strouhal number from 0.02 to 1. Additionally, Nu reduces nearly 27% by enhancing solid to fluid conductivity ratio from 0.5 to 15; however, for solid to fluid conductivity ratio greater than 15, enhancing ksf has no effect on the convective heat transfer [11]. Wang and Zhang conducted numerical simulation on convective heat transfer in turbulent pulsatile flow with large velocity amplitudes of oscillation in a pipe at constant temperature boundary condition at the wall. Their results showed that Womersley number is an essential parameter in pulsatile flow behavior and heat transfer characteristics. Their analysis demonstrated two essential mechanisms of the Nu number augmentation: the larger velocity and the flow setback during a period of the flow oscillation [12]. Ellahi et al proposed a model for analysis of oscillating flow in rotating disk [13].

Jo and Kim analyzed pulsating flow in a channel with parallel-plate, in which a sinusoidal wall temperature boundary condition was imposed on outer surface. They used spectral method to solve the solid and fluid energy equations. They claimed that the convection heat transfer enhances as Re augments with a fixed Peclet number when Reynolds and Peclet number are greater than 1. Their findings illustrated when the dimensionless thermal thickness is less than 0.01; wall heat conduction can be ignored [14]. Zhang et al. studied numerically laminar flow heat transfer in pipes with thick wall in fully developed region. The results show that Nu number is more affected by the ratio of solid-to-fluid thermal conductivity and enhancing wall thickness and the reducing ksf could vary the inner wall surface boundary condition to the constant heat flux boundary condition when $ksf < 25$ [15]. Thus, Satish and Venkatasubbaiah conducted a numerical analysis of turbulent flow in channel with moving plate with considering conjugate heat transfer of fluid and solid. They demonstrated that the temperature between solid and fluid interface reduces, and average Nu number enhances with increasing Reynolds number. Their results revealed heat conduction in solid wall thickness could considerably change the Nusselt

number in channel flows [16]. Meng et al. performed numerical simulation to study solid to fluid thermal interaction in pulsating flow with high-frequency inlet velocity by using Lattice Boltzmann method with different outer wall temperatures. It has been determined the averaged heat fluxes of the pulsatile flow in one period are nearly equal to pure heat conduction in a condition with low-pressure amplitudes and comparatively low-frequency pulsations [17]. Mathie et al. applied simple semi-analytical 1-D model to solve fluid and solid thermal coupling in time-varying inlet velocity. They claimed the model could predict fluid flow and heat transfer behavior in the re-attached and separated flow of a turbulent boundary layer behind a backward-facing step [18]. M. Sheikholeslami et al. applied Laplace transform to study oscillation effect on skin friction coefficient and Nusselt number. They claimed Nu enhances with volume fraction [19]. Zin et al. investigated the same physics in the presence of magnetic field. They showed that magnetic force could suppress fluid flow [20].

Conjugate heat transfer in pulsatile flow is a real running condition in many natural and industrial phenomena. However, up to now, numerous investigations have been conducted to analyze pulsatile flow in tube and channels with wall heat conduction; there is no study concerned with conjugate pulsating flow in ribbed tube. As it was pointed out in literature review, pulsating flow heat transfer is controversial issue needing special attention. The aim of this paper is to study the effects of the pulsation and ribs in heat transfer of tube with solid wall heat conduction. To this purpose, 2D axisymmetric geometry with weakly compressible flow is considered to simulate the pulsatile conjugate heat transfer.

2. Mathematical model

Simulations are carried out on two-dimensional axisymmetric tube. The outer diameter, inner diameter, and length of tube are R_o , R_i and L , respectively. The physical domain with wall thickness of $R_o - R_i$ is depicted in Fig. 1. For modeling the problem, the following assumptions have been employed: (1) the fluid flow is incompressible and laminar (2) the gas is ideal (3) radiation heat transfer and body forces are neglected. Non-dimensional form of Navier-Stokes and energy equation in cylindrical coordinate were used to model the heat transfer and fluid flow [12]:

$$\text{Continuity} \\ \frac{Wo^2}{\pi Re} \frac{\partial \rho_f}{\partial t^*} + \frac{1}{r^*} \frac{\partial (rv^*)}{\partial r^*} + \frac{\partial u^*}{\partial x^*} = 0 \quad (1)$$

$$\text{Momentum-r} \\ \frac{Wo^2}{\pi Re} \frac{\partial u^*}{\partial t^*} + \frac{1}{r^*} \frac{\partial (ru^*v^*)}{\partial r^*} + \frac{\partial (u^*u^*)}{\partial x^*} \\ = -\frac{\partial p^*}{\partial x^*} + \frac{2}{Re} \frac{1}{r^*} \frac{\partial}{\partial r^*} \left(r^* \frac{\partial u^*}{\partial r^*} \right) \\ + \frac{2}{Re} \frac{\partial}{\partial x^*} \left(\frac{\partial u^*}{\partial x^*} \right) \quad (2)$$

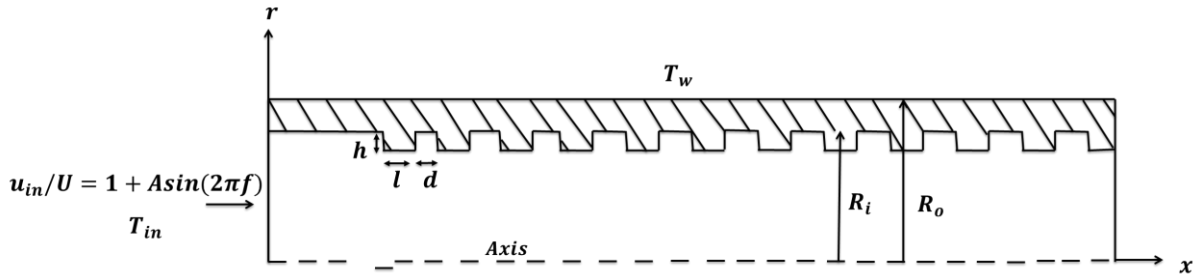


Figure 1. Physical model and boundary condition of numerical simulation

$$\begin{aligned}
 & \text{Momentum-x} \\
 & \frac{Wo^2}{\pi Re} \frac{\partial v^*}{\partial t^*} + \frac{1}{r^*} \frac{\partial (rv^*v^*)}{\partial r^*} + \frac{\partial (u^*v^*)}{\partial x^*} \\
 & = -\frac{\partial p^*}{\partial r^*} + \frac{2}{Re} \frac{1}{r^*} \frac{\partial}{\partial r^*} \left(r^* \frac{\partial v^*}{\partial r^*} \right) \\
 & + \frac{2}{Re} \frac{\partial}{\partial x^*} \left(\frac{\partial v^*}{\partial x^*} \right) - \frac{2}{Re} \frac{2v^*}{r^{*2}}
 \end{aligned} \tag{3}$$

$$\begin{aligned}
 & \text{Fluid Energy} \\
 & \frac{Wo^2}{\pi Re} \frac{\partial T^*}{\partial t^*} + \frac{1}{r^*} \frac{\partial (rv^*T_f^*)}{\partial r^*} + \frac{\partial (u^*T_f^*)}{\partial x^*} \\
 & = \frac{2}{Pr Re} \frac{1}{r^*} \frac{\partial}{\partial r^*} \left(r^* \frac{\partial T^*}{\partial r^*} \right)
 \end{aligned} \tag{4}$$

$$\begin{aligned}
 & \text{Solid Energy} \\
 & \frac{Wo^2}{\pi Re} \frac{\partial T^*}{\partial t^*} = \frac{2}{Re Pr} \frac{\partial}{\partial x^*} \left(\frac{\partial T^*}{\partial x^*} \right) \\
 & + \frac{2}{Pr Re} \frac{1}{r^*} \frac{\partial}{\partial r^*} \left(r^* \frac{\partial T^*}{\partial r^*} \right)
 \end{aligned} \tag{5}$$

The above equations are non-dimensionalized by parameters defined as follows:

$$\begin{aligned}
 r^* &= \frac{r}{R}, & x^* &= \frac{x}{R}, & t^* &= \frac{\omega t}{2\pi}, \\
 p^* &= \frac{p}{\rho U^2}, & v^* &= \frac{v}{U}, & u^* &= \frac{u}{U},
 \end{aligned} \tag{6}$$

$$Re = \frac{UD}{\nu}, T = \frac{T - T_w}{T_{in} - T_w}, Wo = R \sqrt{\frac{\omega}{\nu}}$$

Control Volume Finite volume method (CVFVM) is applied to discretize the continuity, momentum, and energy equations. The detail about the discretization technique can be found in [21]. Second-order implicit three-time level was implemented to discretize the unsteady term in Navier-Stokes and energy equation, which leads to following approximation:

$$\frac{\rho \Delta V}{2 \Delta t} (3u_p - 4u_p^o + u_p^{oo}) \tag{7}$$

By rearranging the equation as follows:

$$\begin{aligned}
 & A_p^t u_p - Q_u^t \\
 & A_p^t = \frac{3\rho \Delta V}{2 \Delta t}, \quad Q_u^t = \frac{\rho \Delta V}{2 \Delta t} (4u_p^o - u_p^{oo})
 \end{aligned} \tag{8}$$

Which u_p^o and u_p^{oo} in above equations are velocities in previous and two previous time levels, respectively. Additionally, convective fluxes of x-momentum equation

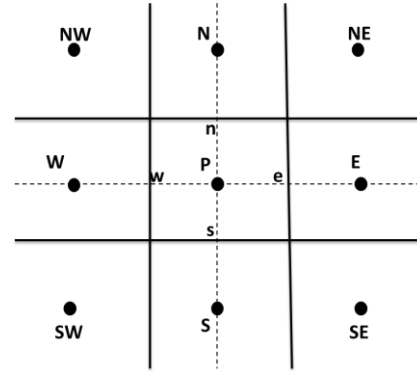


Figure 2. A selected control volume and collocated arrangement of grid

passed from east face of control volume illustrated in Fig. 2 can be calculated by:

$$\begin{aligned}
 & F_e^c = \dot{m}_e u_e \\
 & u_e = (\rho u)_e \Delta y \\
 & F_e^c = \begin{cases} \max(\dot{m}_e, 0) u_p + \min(\dot{m}_e, 0) u_E \\ \dot{m}_e (1 - \lambda_e) u_p + \dot{m}_e \lambda_e u_E \end{cases} \tag{9} \\
 & \lambda_e = \frac{x_e - x_p}{x_E - x_p}
 \end{aligned}$$

Similar expression for the fluxes through other faces of control volume results in the succeeding coefficients in algebraic equation for central and upwind schemes, respectively. For the case of central scheme [22]:

$$\begin{aligned}
 & A_E^c = \dot{m}_e \lambda_e, \quad A_W^c = \dot{m}_w \lambda_w \\
 & A_N^c = \dot{m}_n \lambda_n, \quad A_S^c = \dot{m}_s \lambda_s \\
 & A_P^c = -(A_E^c + A_W^c + A_N^c + A_S^c)
 \end{aligned} \tag{10}$$

In addition, for upwind scheme:

$$\begin{aligned}
 & A_E^c = \min(\dot{m}_e, 0), \quad A_W^c = \min(\dot{m}_w, 0) \\
 & A_N^c = \min(\dot{m}_n, 0), \quad A_S^c = \min(\dot{m}_s, 0) \\
 & A_P^c = -(A_E^c + A_W^c + A_N^c + A_S^c)
 \end{aligned} \tag{11}$$

The relation for A_P^c is derived with applying the continuity condition [23]:

$$\dot{m}_e + \dot{m}_w + \dot{m}_n + \dot{m}_s = 0 \tag{12}$$

With applying the central difference scheme to discretize the diffusion term, the following expression is derived:

$$F_e^d = \left(\mu \frac{\partial u}{\partial x} \right)_e \Delta y = \frac{\mu_e S_e}{x_E - x_p} (u_E - u_p) \tag{13}$$

$$A_E^d = -\frac{\mu_e S_e}{x_E - x_P}, \quad A_W^d = -\frac{\mu_w S_w}{x_P - x_W}$$

$$A_N^d = -\frac{\mu_n S_n}{x_N - x_P}, \quad A_S^d = -\frac{\mu_s S_s}{x_P - x_S}$$

The system of algebraic equation must be diagonally dominant to avoid divergence in iterative solvers. Central difference discretization of convective term in momentum and energy equations may result in system of linear algebraic equations that is not dominant in diagonal. One approach to compel dominance of diagonal in systems of linear algebraic equations is usage the deferred correction technique proposed by Kholsa and Rubin [24].

$$F_e^c = \dot{m}_e u_e^{UDS} + \dot{m}_e (u_e^{CDS} - u_e^{UDS})^{m-1} \quad (14)$$

Where superscripts, CDS, and UDS in equation 14 denote central differencing and upwind scheme estimates, respectively. The rate of convergence in this approach is almost similar to upwind scheme [25].

The pressure gradient will be treated as a source term and is computed as:

$$Q_P^u = -(p_e S_e - p_w S_w)^{m-1} \quad (15)$$

The detail about pressure term treatment in momentum equation can be found in [25]. Finally, the system of linear equations is as follows:

$$A_P^u u_P + A_E^u u_E + A_W^u u_W + A_N^u u_N + A_S^u u_S = Q_P^u$$

$$A_E^u = A_E^c + A_E^d, \quad A_W^u = A_W^c + A_W^d$$

$$A_N^u = A_N^c + A_N^d, \quad A_S^u = A_S^c + A_S^d \quad (16)$$

$$A_P^u = A_P^c - (A_E^u + A_W^u + A_N^u + A_S^u)$$

$$Q_P^u = Q_u^p + Q_u^c + Q_u^t$$

Where the source term Q_u^c is calculated with:

$$Q_u^c = [(F_u^c)^{UDS} - (F_u^c)^{CDS}]^{m-1} \quad (17)$$

In the case of cylindrical coordinate system, the term $\mu \Delta V / r_p^2$ should be added to A_P^u in radial momentum equation. The boundary condition can be formulated as follows:

$$r = 0, \quad 0 \leq x \leq L, \quad \frac{\partial T_f}{\partial r} = 0,$$

$$\frac{\partial u}{\partial r} = 0$$

$$r = R_i, \quad 0 \leq x \leq L,$$

$$-k_f \frac{\partial T_f}{\partial r} = -k_s \frac{\partial T_s}{\partial r}, \quad T_f = T_s, \quad v = 0,$$

$$u = 0 \quad (18)$$

$$r = R_o, \quad 0 \leq x \leq L, \quad T_s = T_w$$

$$x = 0, \quad 0 \leq r \leq R_i, \quad T_f = T_{in},$$

$$u = U(1 + A \sin(2\pi f))$$

$$x = L, \quad 0 \leq r \leq R_i, \quad \frac{\partial T_f}{\partial x} = 0,$$

$$\frac{\partial u}{\partial x} = 0$$

The linear algebraic equation is solved by the Stone's SIP solver. Stone's method, also known as the strongly implicit procedure or SIP, is an algorithm for solving a sparse linear system of algebraic equations. The method utilizes an incomplete LU decomposition, which approximates the exact LU decomposition to find an iterative solution for the system of linear algebraic

equations. Bulk temperature, Nusselt number, Reynolds and Prandtl numbers are defined as follows:

$$T_{bf} = \frac{\int_0^{R_i} u T_f r dr}{\int_0^{R_i} u r dr},$$

$$Nu_{x,t} = \frac{2}{T_w - T_{fb}} \left(\frac{\partial T_f}{\partial r} \right)_{r=R_i}, \quad (19)$$

$$Re = \frac{UD_i}{\nu},$$

$$Pr = \frac{c_{p,f} \mu_f}{k_f}$$

The time-averaged and space averaged Nusselt number can be calculated according to the following equations [12]:

$$\overline{Nu}_x = \frac{\int_0^T |Nu_{x,t}| dt}{\int_0^T dt},$$

$$\overline{Nu}_t = \frac{\int_0^L |Nu_{x,t}| dx}{\int_0^L dx}, \quad (20)$$

$$\overline{\overline{Nu}} = \frac{\int_0^L \int_0^T |Nu_{x,t}| dt dx}{\int_0^L \int_0^T dt dx}$$

The coupling between solid and fluid energy equations can be satisfied by two approaches. In the first approach known as conjugate scheme, the whole energy equations of the solid and fluid is solved as single set of equation and the heat flux and temperature equality are satisfied implicitly at the interface. In the second approach known as coupled scheme, the energy equations are solved independently. The first method is employed in the simulation because it is more stable.

3. Results and discussion

3.1. Validation of the numerical simulation

To model conjugate heat transfer of pulsatile flow in the tube, a code was developed and compiled in Fortran 90. The grid independence check is necessary to confirm the verification and accuracy of the numerical simulation results. Four sets of grid numbers are considered to investigate the mesh density effect on the numerical computation. The mesh number are almost 6250, 9000, 16000, and 25000. The velocity on the axis of the tube of the four sets with different grid numbers is demonstrated in Fig. 3. The implemented mesh number in the computational domain is about 16000 in order to save computer run time and making a balance between computational accuracy and costs.

The accuracy of the present method of solution and the numerical model has been verified with the numerical results, which is published in the scientific literature. For the verification of the numerical method and the computational model, two numerical simulations at the different operating conditions and geometric sizes, as presented in [26] and [15] are conducted. Zhao and Cheng numerically investigated oscillating flow created with a

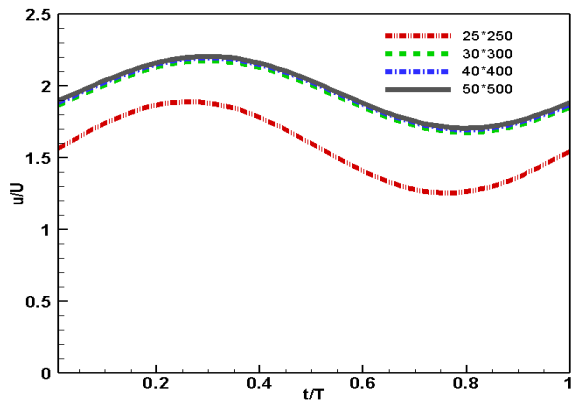


Figure 3. Velocity variation in one cycle on the axis of the tube at fully developed region

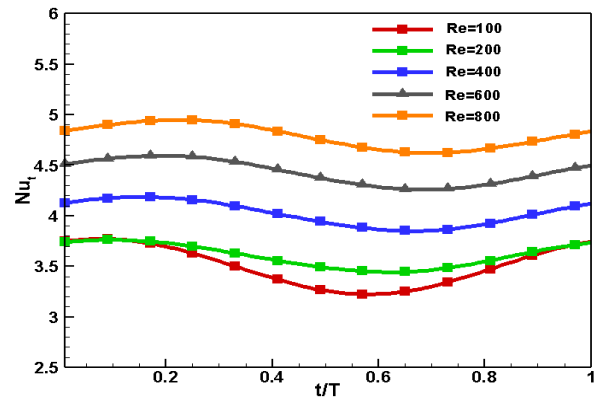


Figure 6. Averaged Nusselt number versus time at different Reynolds number

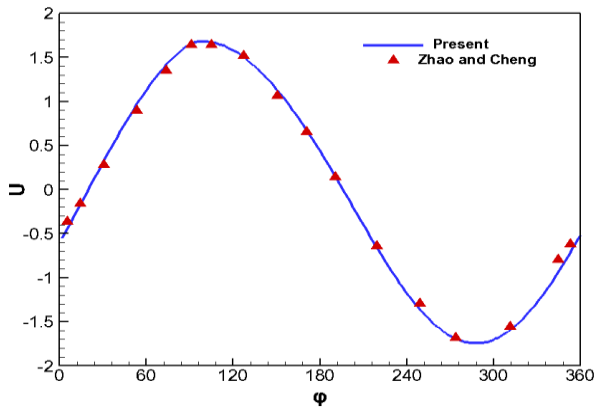


Figure 4. Comparison of temporal u-velocity with Zhao and Cheng [26] for $L/D=40$, $Re_w=64$ and $A_0=15$ at $X/D=6.2$

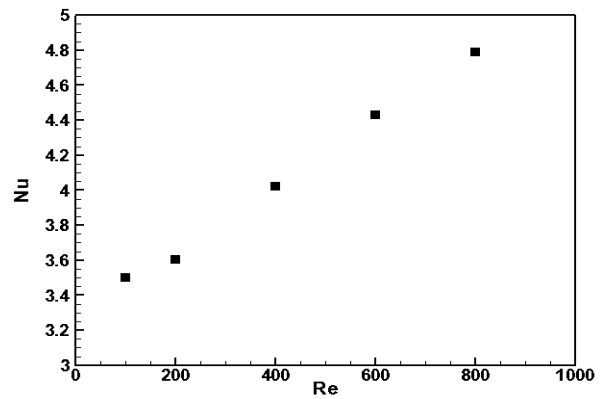


Figure 7. Variation of cycled averaged Nusselt number versus Reynolds number

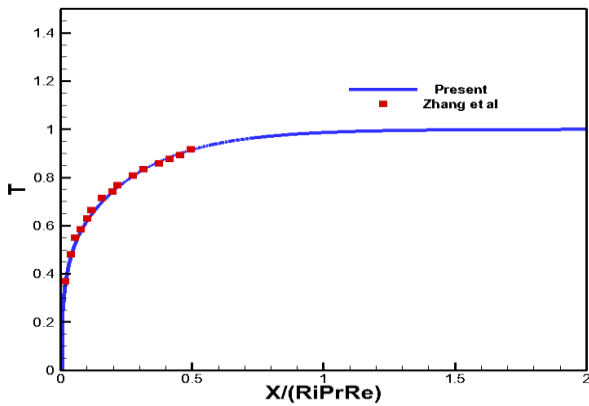


Fig. 5. Variation of temperature at the inner surface of the tube in comparison with Zhang et al. [15] at $k_{sf}=1.0$, $\delta/R_i=0.84$, $Pr=1.0$ and $Re=50$

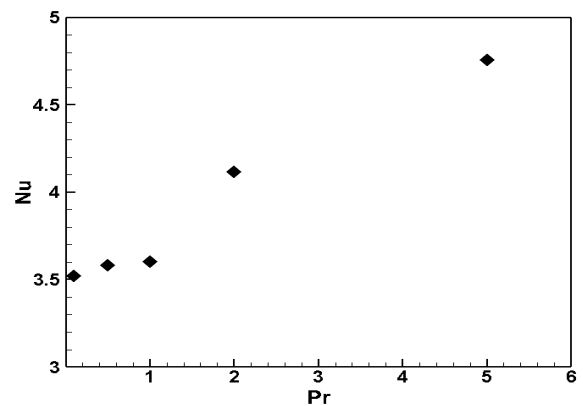


Figure 8. Variation of averaged Nusselt number versus Prandtl number

pressure wave generator piston in tube with constant wall temperature. The comparison with their results is presented in Fig. 4. It can be seen the numerical computation of the developed code agrees well with Zhao's results. The results were also compared to [15], in order to get confident about the validation of the results of the code by considering the energy equation. Zhang et al. carried out numerical analysis on the conjugate heat transfer of solid and fluid in the steady-state flow at the

tube. There is good agreement between the code results with Zhang's numerical simulation.

In the proceeding, important parameters will be studied in the conjugate heat transfer of pulsating flow. These parameters are Reynolds number, Prandtl number, Womersley number, wall thickness ratio, the geometry of rib in the tube, and amplitude of velocity.

3.2. Effect of Reynolds number on Nusselt number

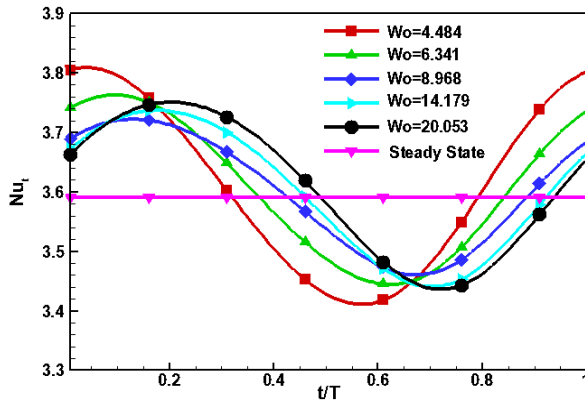


Figure 9. Cycled averaged Nusselt number variation versus time at different Womersley number

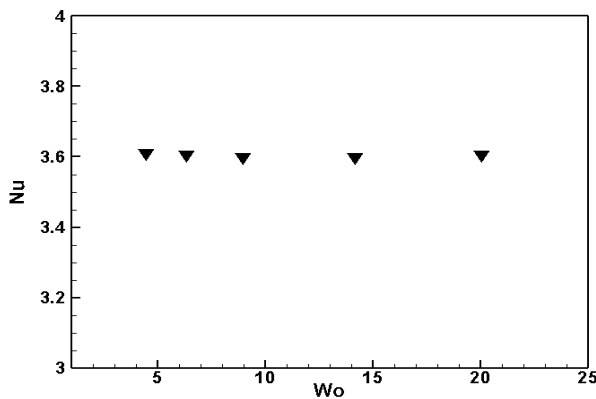


Figure 10. Cycled averaged Nusselt number variation versus Womersley number

The variation of Nu number with Re number at $Wo=6.341$ and $A=0.2$ in one period of pulsatile flow is demonstrated in Fig. 6. The instantaneous Nu number changes sinusoidally with time. It is clearly seen that Reynolds number strongly influences the heat transfer augmentation in pulsatile flow. Averaged Nusselt number is also depicted in Fig. 7. Nu increases almost 36.8% by enhancing Re from 100 to 800. The heat transfer rate linearly increases since the difference between wall and bulk temperature is enhancing. In other words, the higher velocity of fluid flow with increasing Re number causes higher collision among the fluid particles. Due to higher collision among fluid particles, heat transition rate improves.

3.3. Effect of Prandtl number on Nusselt number

The variation of averaged Nu on Pr number is depicted in Fig. 8. Nu increases sharply by Pr increment. Nu increases almost 35% by Pr enhancement from 0.1 to 5. With the increment in the Prandtl number the Nusselt number also increases, so the convection heat transfer rate also increases. Prandtl number is defined with the ratio of momentum diffusivity to the thermal diffusivity. So with the increase in Prandtl number signifies that the momentum diffuses quickly, and the velocity boundary

layer is comparatively less thick than the thermal boundary layer, which in turn means more heat transfer by the bulk motion (also called advection), this means convection is dominant than conduction.

3.4. Effect of Womersley number on Nusselt number

The temporal variation of Nu versus Womersley number is depicted in Fig. 9. It seems pulsatile flow at different Wo numbers does not affect convective heat transfer coefficient. Nu in pulsatile flow oscillates around steady-state Nu number. Averaged Nu number in different Wo numbers is also depicted in Fig. 10. As can be seen, Nu remains constant by varying Wo number. Based on Nandi and Chattopadhyay's works, it was realized that imposing oscillating velocity at the inlet of the tube can provide improved performance of convective heat transfer at different amplitudes of pulsation. However, Mathie et al. [27] found reduction of Nu number in their analysis of heat transfer in unsteady compressible flow. In present paper, it is elucidated that Wo has no effect on Nu number and heat transfer in ribbed-tube which admits Matinelli et al. [7] and Genin et al. [8] results.

3.5. Effect of wall thickness ratio on Nusselt number

Nu enhances almost 19% by increasing wall thickness ratio from 0.125 to 1. It is remarkable that Sparrow and Patankar conducted a comprehensive investigation for thermally developed flow in duct and tube with different boundary conditions for energy equation with negligible wall thickness ratio [28]. They concluded constant wall temperature and the constant heat flux are two extreme boundary conditions for Nusselt number in fully developed flow, and by increasing Bi number, Nu varies from constant heat flux with $Nu=4.36$ to constant wall temperature $Nu=3.66$ asymptotically.

In the present paper, our numerous simulations showed that as wall thickness ratio enhances, the convective heat transfer coefficient or Nu number at inner face of a tube wall with constant temperature imposed at the outside of the tube will encounter a boundary condition transformation from Dirichlet to Neumann boundary condition.

The temperature at the common face of fluid and solid wall reduces with enhancement in wall thickness due to increment of conductive thermal resistance or reduction in conductive heat transfer at the solid wall. As temperature of the common face between solid and fluid declines, the convective heat transfer coefficient and the Nu number augments to preserve the energy balance between the inner and outer surfaces of solid region. Hereafter, the Nusselt number improves with thickening the solid wall at a constant Prandtl Reynolds number.

For evaluating the influence of solid wall heat conduction on Nu number and convective heat transfer in the tube, Guo and Li proposed a non-dimensional parameter (M). They defined M [29]:

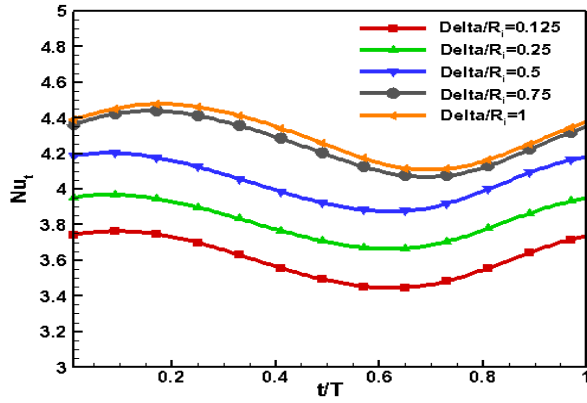


Figure 11. Cycled averaged Nusselt number variation versus time at different wall thickness ratio

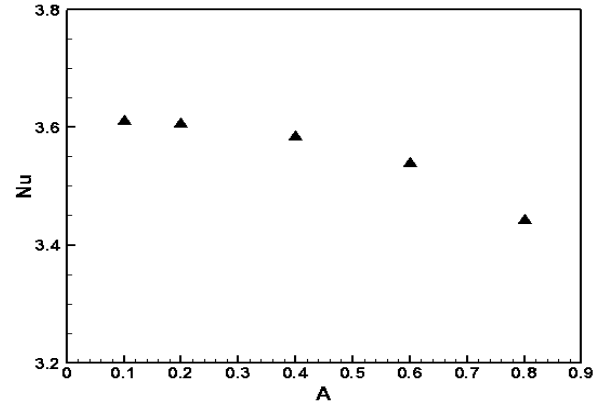


Figure 13. Cycled averaged Nusselt number variation versus amplitude of pulsating velocity

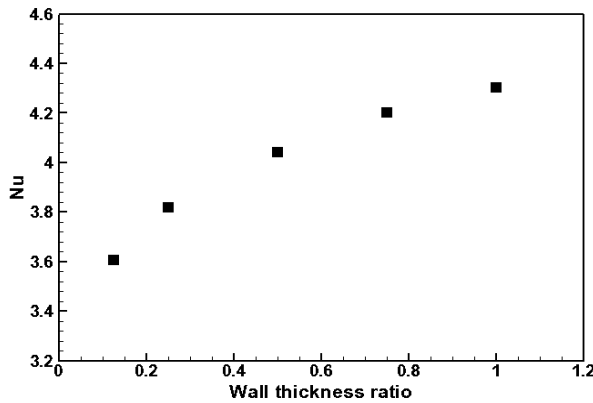


Figure 12. Cycled averaged Nusselt number variation versus wall thickness ratio

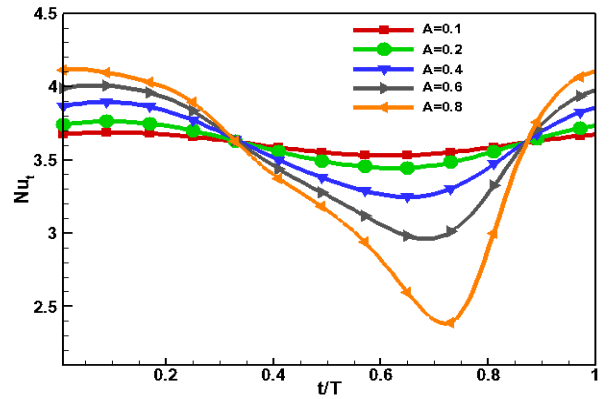


Figure 14. Cycled averaged Nusselt number variation versus time at different amplitude of pulsating velocity

$$M = \frac{\phi_{cond}}{\phi_{conv}} = \frac{(R_o^2 - R_i^2)k_s \Delta T_s / L_h}{R_i^2 \rho c_p u_{ave} \Delta T_l} \quad (21)$$

The non-dimensional number (M) is redefined by Maranzana as follow [30]:

$$M = \frac{\phi_{cond}}{\phi_{conv}} = \frac{r^2 NTU}{Bi} \quad (22)$$

It was noted that with M less than 0.01 wall thermal inertia can be neglected. However, they assumed that the heat transfer coefficient is constant at the inner wall of the tube; therefore, their results is not applicable to the problems where local heat transfer coefficient is a varying parameter rather than a given fixed value. Other equations were proposed by Cotton and Jackson [31] and Faghri and Sparrow [32]. In all equations it is clear that by increasing solid wall thickness, axial heat conduction and wall thermal inertia becomes more predominant. It can be deduced from Fig. 11 and Fig. 12 that by enhancing solid wall thickness ratio, flow in the tube will not sense outside wall boundary condition and inner wall boundary condition will approach toward constant wall heat flux.

3.6. Effect of amplitude of the inlet velocity on Nusselt number

In order to investigate the effect of velocity amplitude on the heat transfer coefficient five amplitudes of A=0.1,

0.2, 0.4, 0.6, 0.8 were adopted. Averaged Nu number versus velocity amplitude is demonstrated in Fig. 13. Nu number decreases by almost 4.7% by increasing velocity amplitude from 0.1 to 0.8. Because flow reversal increases by enhancing velocity amplitude and hence fluid resident time in tube increases and this causes reduction in the difference between the bulk temperature and the inner wall temperature. This will consequence in reduction of the temperature gradient at the fluid and solid interface, which will result in Nu number decrease. The time variation of Nu number in one period is depicted in Fig. 14. It can be observed by decreasing velocity Nu decreases, and for velocity amplitude greater than 0.4, Nu reduces rapidly after $t=T/2$.

3.7. Effect of height of ribs in the tube on Nusselt number

Nu number decrease with increasing the height of rib in the tube. As it is depicted in Fig. 15 Nu decreases by 12.7%. Temperature difference between inner surface of the ribbed tube and bulk temperature increases and gradient of temperature at the interface of fluid and solid wall also enhances by increasing height ratio of ribs, but the augmentation of bulk temperature difference with interface temperature dominants and results in reduction of Nu number.

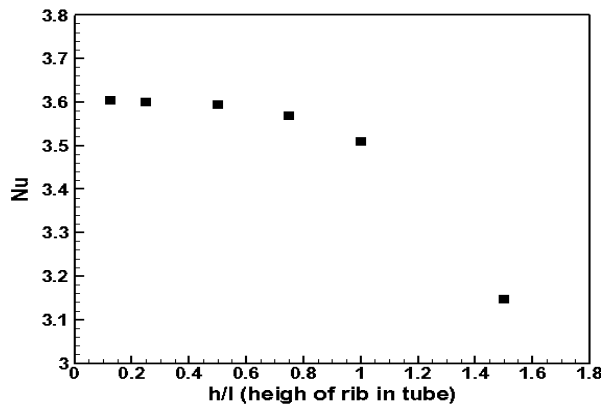


Figure 15. Cycled averaged Nusselt number variation versus height of rib ratio

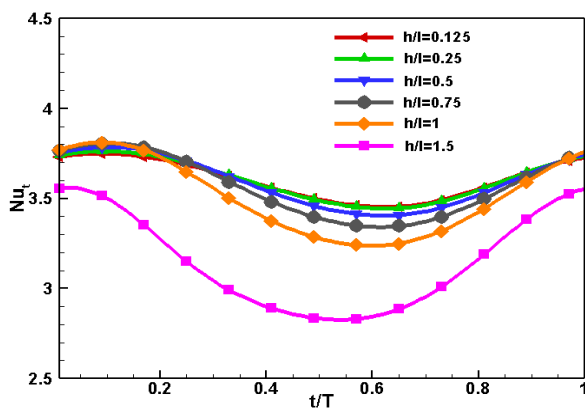


Figure 16. Cycled averaged Nusselt number variation versus time at different rib height ratio

Conclusion

Conjugate heat transfer of pulsatile flow in ribbed tube was investigated by solving non-dimensional Navier-Stokes and energy equations in cylindrical coordinate system with finite volume technique (FVM). The well-known SIMPLE method of Patankar was adopted for dealing the coupling between pressure and velocity, and checker-board in collocated arrangement of grids was avoided by implementing Rie and Chow interpolation method. It was elucidated that increasing Wo number has no effect on the Nu number. Nu enhances almost 35% by augmentation of Pr number from 0.1 to 5, and for Pr number greater than 1, Nu enhances sharply. Solid wall thickness is a salient parameter in conjugate heat transfer of pulsating flow. By increasing solid wall thickness ratio from 0.125 to 1, Nu augmented 19% due to the boundary condition transformation from Dirichlet to Neumann. It was also depicted that Nu number decreases almost 4.7% by increasing velocity amplitude from 0.1 to 0.8 because the difference between the bulk temperature and the inner wall temperature and the temperature gradient at the solid and fluid interface reduces. Additionally, increasing height of ribs in the tube can result in Nu number reduction.

Nomenclature

| | |
|-----------|------------------------------|
| A | Velocity amplitude |
| $c_{p,f}$ | Fluid specific heat |
| $c_{p,s}$ | Solid specific heat |
| c_f | Coefficient of pressure drop |
| d | Distance of ribs in tube |
| D_i | Inner diameter of tube |
| f | Frequency |
| h | Height of ribs in tube |
| k_f | Fluid conductivity |
| k_s | Solid conductivity |
| l | Length of ribs in tube |
| L | Tube length |
| Nu | Nusselt number |
| Pr | Prandtl number |
| p | Pressure |
| Re | Reynolds number |
| R_i | Inner radius of tube |
| R_o | Outer radius of tube |
| T_{in} | Inlet temperature |
| T_w | Wall temperature |
| T_f | Fluid temperature |
| T_s | Solid temperature |
| u_{in} | Inlet velocity |
| U | Inlet velocity magnitude |
| Wo | Womersley number |
| δ | Wall thickness |
| μ | Dynamic viscosity |
| ρ_f | Fluid density |
| ρ_s | Solid density |
| τ_w | Wall shear stress |

Conflict of Interest

The authors declare that They have no conflict of interest.

References

- [1] Sinha, A. and Misra, J. C. (2012) 'Numerical study of flow and heat transfer during oscillatory blood flow in diseased arteries in presence of magnetic fields', *Applied Mathematics and Mechanics* (English Edition), 33(5), pp. 649–662. doi: 10.1007/s10483-012-1577-8.
- [2] Kardgar, A., Jafarian, A. and Arablu, M. (2016) 'An Eulerian-Lagrangian model to study the operating mechanism of Stirling pulse tube refrigerators', *Scientia Iranica*, 23(1), pp. 277–284. doi:10.24200/sci.2016.3833.
- [3] Kardgar, A. and Jafarian, A. (2020) 'Numerical simulation of turbulent oscillating flow in porous media', *Scientia Iranica*. doi: 0.24200/SCI.2020.52521.2788.
- [4] Yuan, H. et al. (2014) 'Theoretical analysis of wall thermal inertial effects on heat transfer of pulsating laminar flow in a channel', *International Communications in Heat and*

- Mass Transfer. Elsevier Ltd, 53, pp. 14–17. doi:10.1016/j.icheatmasstransfer.2014.02.003.
- [5] Khosravi-Bizhaem, H., Abbassi, A. and Zivari Ravan, A. (2019) 'Heat transfer enhancement and pressure drop by pulsating flow through helically coiled tube: An experimental study', *Applied Thermal Engineering*. Elsevier, 160(April), p. 114012. doi: 10.1016/j.applthermaleng.2019.114012.
- [6] Li, P., Guo, D. and Liu, R. (2019) 'Mechanism analysis of heat transfer and flow structure of periodic pulsating nanofluids slot-jet impingement with different waveforms', *Applied Thermal Engineering*, 152(July 2018), pp. 937–945. doi:10.1016/j.applthermaleng.2019.01.086.
- [7] Martinelli, R. C. et al. (1943) 'Heat transfer to a fluid flowing periodically at low frequencies in a vertical tube', *Trans. Asme*, 65(7), pp. 789–798.
- [8] Genin, L. G. et al. (1993) 'Heat transfer and friction for pulsating water flow in a pipe', *Heat transfer research*. Wiley, 25(2), pp. 193–195.
- [9] Park, J. S., Taylor, M. F. and McEligot, D. M. (1982) 'Heat transfer to pulsating, turbulent gas flow', in *Proceedings of the 7th International Heat Transfer Conference Digital Library*, pp. 105–110.
- [10] Karamercan, O. E. and Gainer, J. L. (1979) 'The effect of pulsations on heat transfer', *Industrial & Engineering Chemistry Fundamentals*. ACS Publications, 18(1), pp. 11–15.
- [11] Kardgar, A. and Jafarian, A. (2016) 'Numerical investigation of oscillating conjugate heat transfer in pulse tubes', *Applied Thermal Engineering*. Elsevier Ltd, 105, pp. 557–565. doi:10.1016/j.applthermaleng.2016.03.045.
- [12] Wang, X. and Zhang, N. (2005) 'Numerical analysis of heat transfer in pulsating turbulent flow in a pipe', *International Journal of Heat and Mass Transfer*, 48(19–20), pp. 3957–3970. doi:10.1016/j.ijheatmasstransfer.2005.04.011.
- [13] Ellahi, R. et al. (2017) 'On boundary layer nano-ferroliquid flow under the influence of low oscillating stretchable rotating disk', *Journal of Molecular Liquids*, 229, pp. 339–345. doi: 10.1016/j.molliq.2016.12.073.
- [14] Jo, J. and Kim, S. J. (2017) 'Conjugate heat transfer by oscillating flow in a parallel-plate channel subject to a sinusoidal wall temperature distribution', *Applied Thermal Engineering*. Elsevier Ltd, 123, pp. 1462–1472. doi:10.1016/j.applthermaleng.2017.05.155.
- [15] Zhang, S. X. et al. (2010) 'Numerical studies of simultaneously developing laminar flow and heat transfer in microtubes with thick wall and constant outside wall temperature', *International Journal of Heat and Mass Transfer*. Elsevier Ltd, 53(19–20), pp. 3977–3989. doi:10.1016/j.ijheatmasstransfer.2010.05.017.
- [16] Satish, N. and Venkatasubbaiah, K. (2016) 'Conjugate heat transfer analysis of turbulent forced convection of moving plate in a channel flow', *Applied Thermal Engineering*. Elsevier Ltd, 100, pp. 987–998. doi: 10.1016/j.applthermaleng.2016.02.076.
- [17] Meng, F., Wang, M. and Li, Z. (2008) 'Lattice Boltzmann simulations of conjugate heat transfer in high-frequency oscillating flows', *International Journal of Heat and Fluid Flow*, 29(4), pp. 1203–1210. doi: 10.1016/j.ijheatfluidflow.2008.03.001.
- [18] Mathie, R., Nakamura, H. and Markides, C. N. (2013) 'Heat transfer augmentation in unsteady conjugate thermal systems - Part II: Applications', *International Journal of Heat and Mass Transfer*. Elsevier Ltd, 56(1–2), pp. 819–833. doi:10.1016/j.ijheatmasstransfer.2012.09.017.
- [19] Sheikholeslami, M., Kataria, H. R. and Mittal, A. S. (2018) 'Effect of thermal diffusion and heat-generation on MHD nanofluid flow past an oscillating vertical plate through porous medium', *Journal of Molecular Liquids*, pp. 12–25. doi: 10.1016/j.molliq.2018.02.079.
- [20] Mohd Zin, N. A., Khan, I. and Shafie, S. (2016) 'The impact silver nanoparticles on MHD free convection flow of Jeffrey fluid over an oscillating vertical plate embedded in a porous medium', *Journal of Molecular Liquids*, 222, pp. 138–150. doi: 10.1016/j.molliq.2016.06.098.
- [21] Zhang, S., Zhao, X. and Bayyuk, S. (2014) 'Generalized formulations for the rhie-chow interpolation', *Journal of Computational Physics*. Elsevier Inc., 258, pp. 880–914. doi: 10.1016/j.jcp.2013.11.006.
- [22] Kardgar, A. (2020) 'Numerical investigation of conjugate heat transfer and entropy generation of MHD natural convection of nanofluid in an inclined enclosure', *International Journal of Numerical Methods for Heat & Fluid Flow*. Emerald Publishing Limited.
- [23] Rezaei, M., Jafarian, A. and Kardgar, A. (2017) 'Numerical investigation of real gas

- effects on a two-stage pulse tube cryocooler performance', *International Journal of Refrigeration*, 82, pp. 106–118. doi: 10.1016/j.jrefrig.2017.06.008.
- [24] Khosla, P. K. and Rubin, S. G. (1974) 'A diagonally dominant second-order accurate implicit scheme', *Computers & Fluids*. Elsevier, 2(2), pp. 207–209.
- [25] Ferziger, J. H. and Peric, M. (2001) *Computational Methods for Fluid Dynamics*. Springer Berlin Heidelberg. Available at: <https://books.google.com/books?id=1D3EQgAACAAJ>.
- [26] Zhao, T. and Cheng, P. (1995) 'A numerical solution of laminar forced convection in a heated pipe subjected to a reciprocating flow', *International Journal of Heat and Mass Transfer*, 38(16), pp. 3011–3022. doi: 10.1016/0017-9310(95)00017-4.
- [27] Mathie, R. and Markides, C. N. (2013) 'International Journal of Heat and Mass Transfer Heat transfer augmentation in unsteady conjugate thermal systems – Part I: Semi-analytical 1-D framework', *International Journal of Heat and Mass Transfer*. Elsevier Ltd, 56(1–2), pp. 802–818. doi:10.1016/j.ijheatmasstransfer.2012.08.023.
- [28] E. M. Sparrow and S. V. Patankar (1977) 'Relationships among boundary conditions and nusselt numbers for thermally developed duct flows', *Journal of Heat Transfer. American Society of Mechanical Engineers(ASME)*, 99, pp. 483--485. doi: 10.1115/1.3450722.
- [29] Guo, Z. and Li, Z. (2003) 'Size effect on single-phase channel flow and heat transfer at microscale', 24, pp. 284–298. doi: 10.1016/S0142-727X(03)00019-5.
- [30] Maranzana, G., Perry, I. and Maillet, D. (2004) 'Mini- and micro-channels: influence of axial conduction in the walls', *International Journal of Heat and Mass Transfer*, 47, pp. 3993–4004. doi: 10.1016/j.ijheatmasstransfer.2004.04.016.
- [31] Cotton, M. A. and Jackson, J. D. (1985) 'The effect of heat conduction in a tube wall upon forced convection heat transfer in the thermal entry region', *Numerical Methods in Thermal Problems*, Pineridge Press, Swansea, 4, pp. 504–515.
- [32] Faghri, M. and Sparrow, E. M. (1980) 'Simultaneous wall and fluid axial conduction in laminar pipe-flow heat transfer', *Journal of Heat Transfer*, 102(1), pp. 58–63.